Electronic Supplementary Material (ESI) for Journal of Materials Chemistry C.

Direct laser patterning of organic semiconductors for high performance OFET-based gas sensors

Li Chen,[a] Yuzhou Hu,[b] Huaxi Huang,[a] Chao Liu,[b] Di Wu,* [a] Jianlong Xia*[a]

[a] Prof. J. Xia, Assoc. Prof. D.Wu, L. Chen, H. X. Huang

School of Chemistry, Chemical Engineering and Life Science, Wuhan University of Technology, No. 122 Luoshi Road, Wuhan 430070, China; State Key Laboratory of Advanced Technology for Materials Synthesis and Processing, Center of Smart Materials and Devices, Wuhan University of Technology, No. 122 Luoshi Road, Wuhan 430070, China.

E-mail: D. Wu. (chemwd@whut.edu.cn); J. Xia. (jlxia@whut.edu.cn)

[b] Prof. C. Liu, Y. Z. Hu

State Key Laboratory of Silicate Materials for Architectures, Wuhan University of Technology, 122 Luoshi Road, Hongshan, Wuhan 430070, China.

Table of contents S2

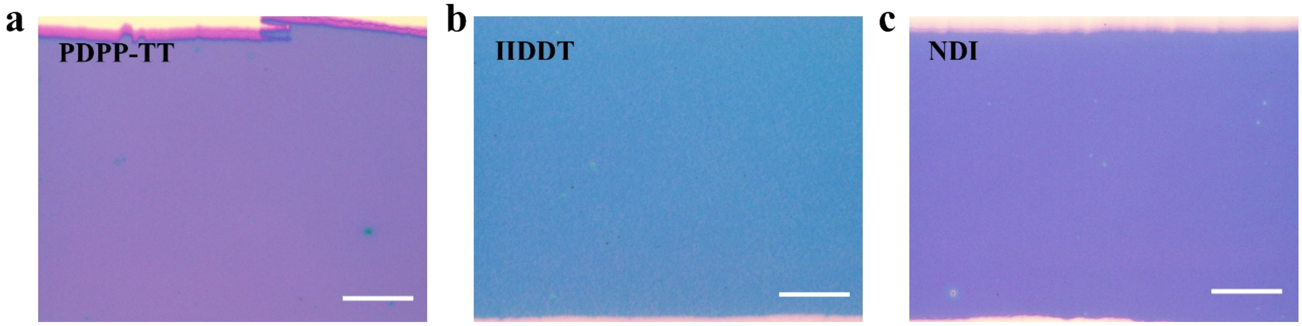

Fig. S1. Optical microscope (OM) images of pristine (a) PDPP-TT, (b) IIDDT and (c) NDI semiconductor films. The scale bar is 10 μm.

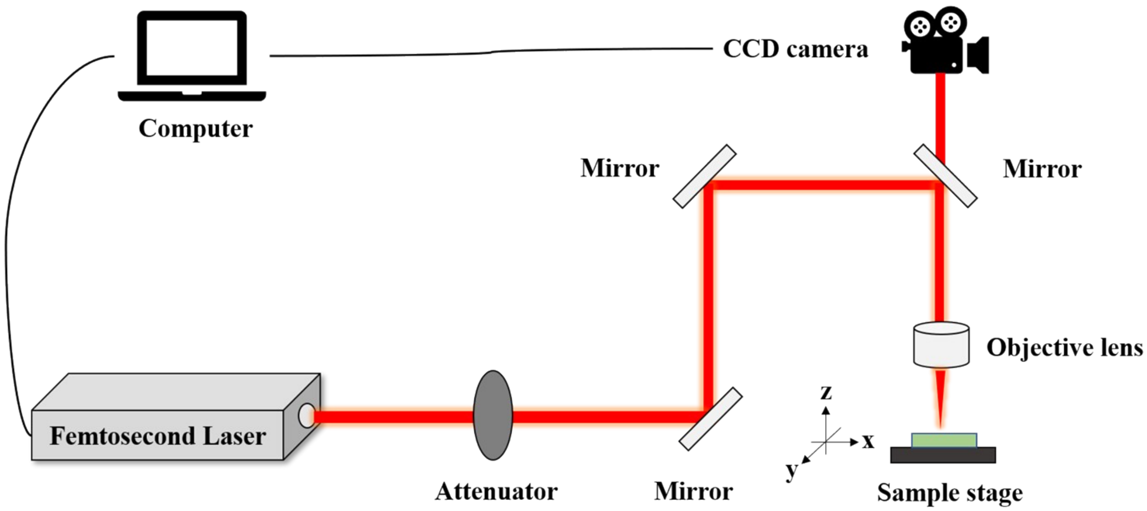

Fig. S2. Schematic diagram of femtosecond micro-fabrication system.

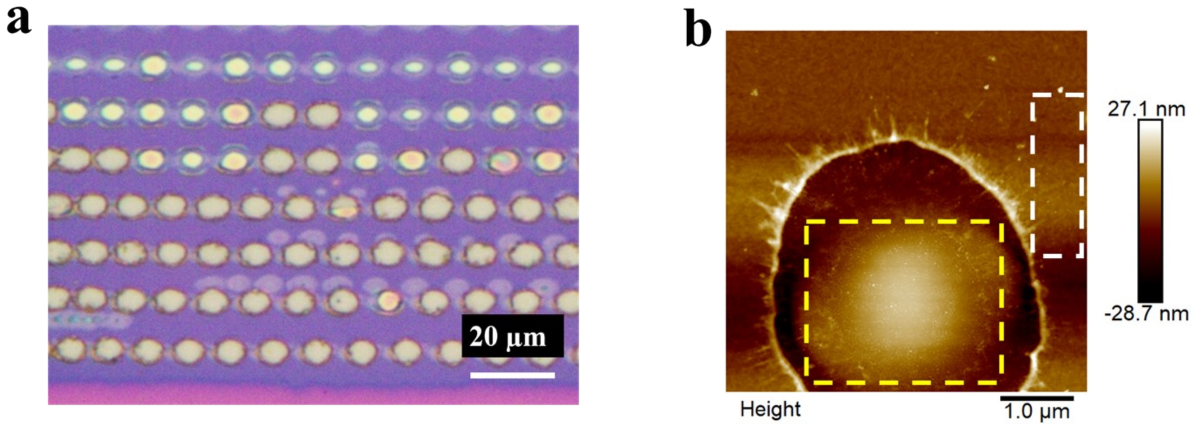

Fig. S3. (a) Optical microscope (OM) image of laser-processed PDPP-TT thin film. The laser beam was focused on the surface of OSC film and the underneath SiO_2 dielectric was obviously damaged. (b) The AFM image of pore pattern. The laser beam with high energy density has triggered the melting and reshaping of SiO_2 dielectric layer, resulting in obvious bulge within the pore pattern (The yellow dashed rectangle region). And this side effect can also affect the morphology of OSC covered region (As shown in white dashed rectangle area).

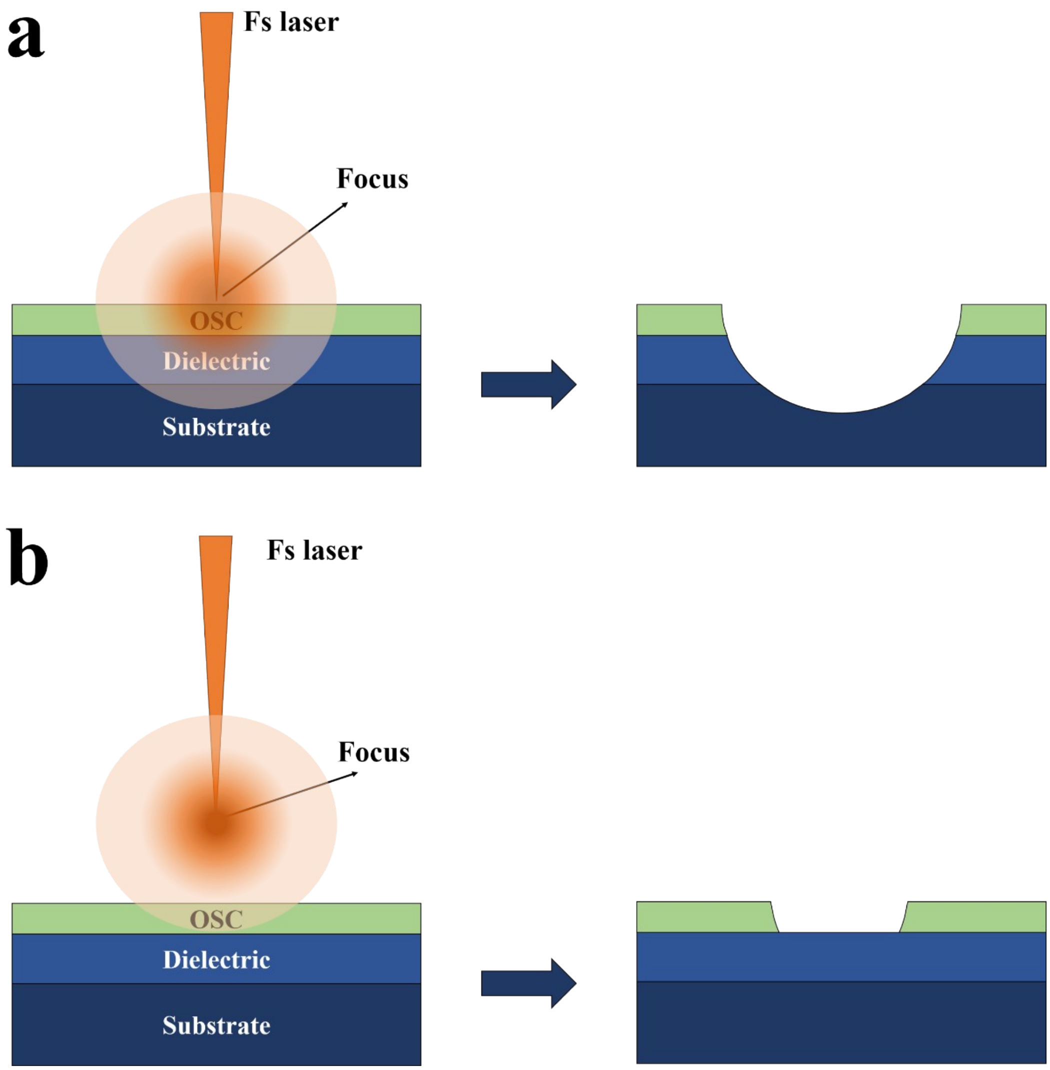

Fig. S4. Schematic diagram of fs laser ablation process. (a) Fs laser fabrication with the focus on OSC surface. (b) Defocusing fs laser fabrication process.

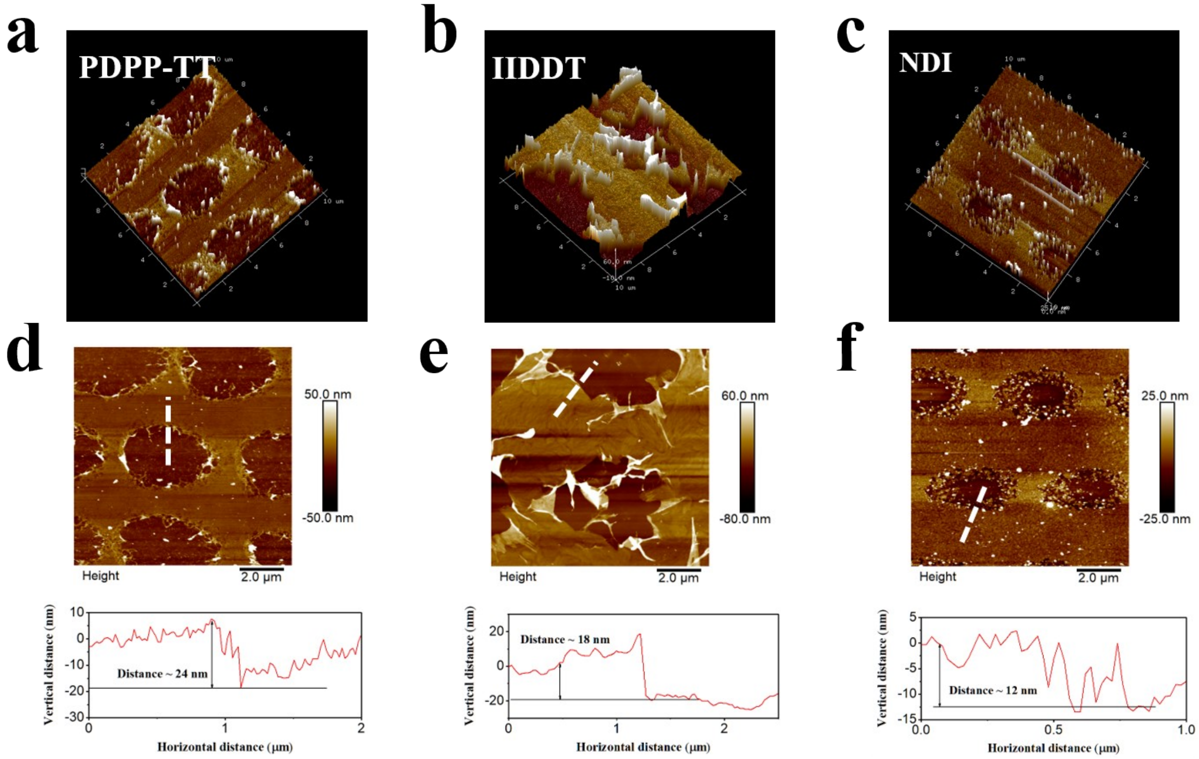

Fig. S5. Surface morphology analysis. (a-c) 3D AFM images of patterned films for (a) PDPP-TT, (b) IIDDT and (c) NDI materials. (d-f) AFM image and height profile for selective line of (d) PDPP-TT, (e) IIDDT and (f) NDI based patterned OSC films.

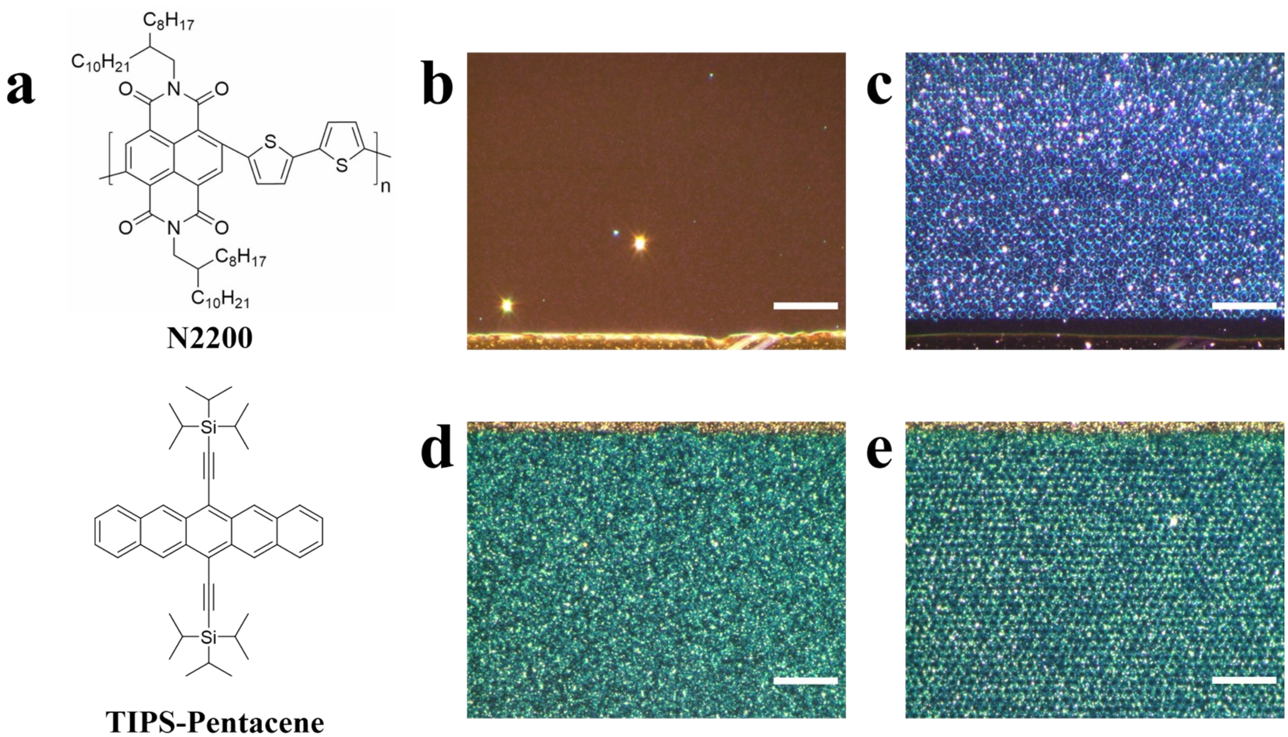

Fig. S6. (a) Chemical structures of N2200 and TIPS-Pentacene. (b-e) Optical images of pristine and patterned films of (b,c) N2200 and (d,e) TIPS-Pentacene materials. The scale bar is 10 μm.

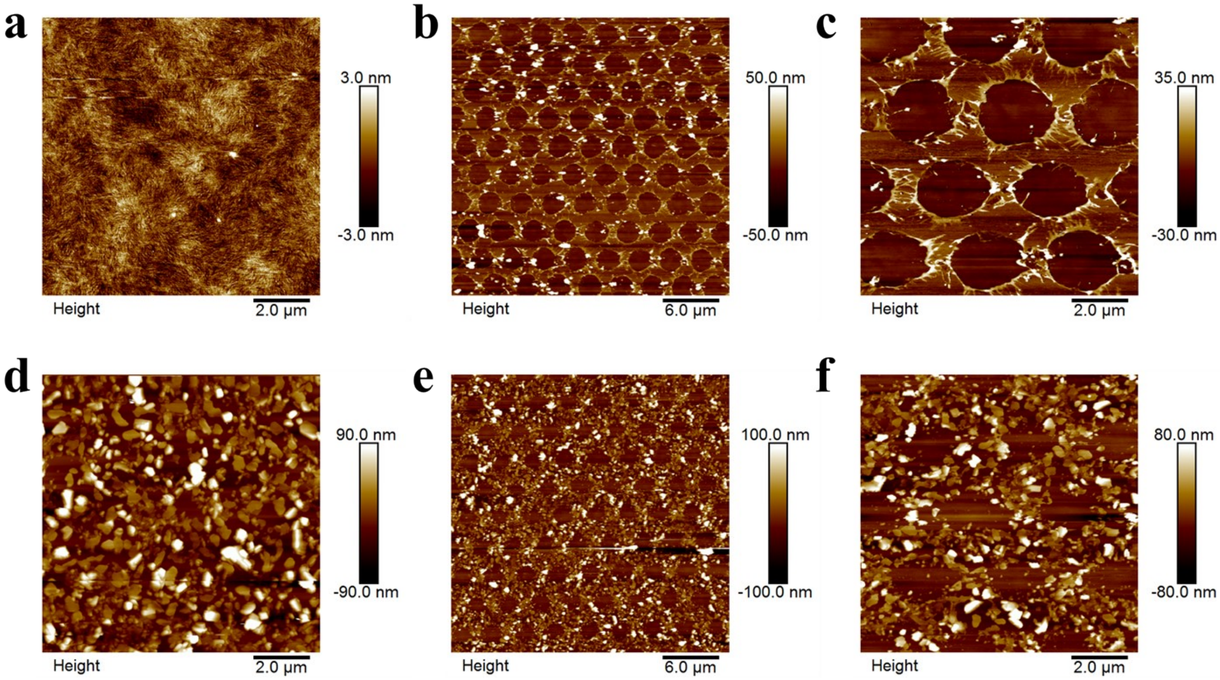

Fig. S7. (a-c) AFM height images of (a) pristine and (b,c) patterned N2200 films. (d-f) AFM height images of (d) pristine and (e,f) patterned TIPS-Pentacene films.

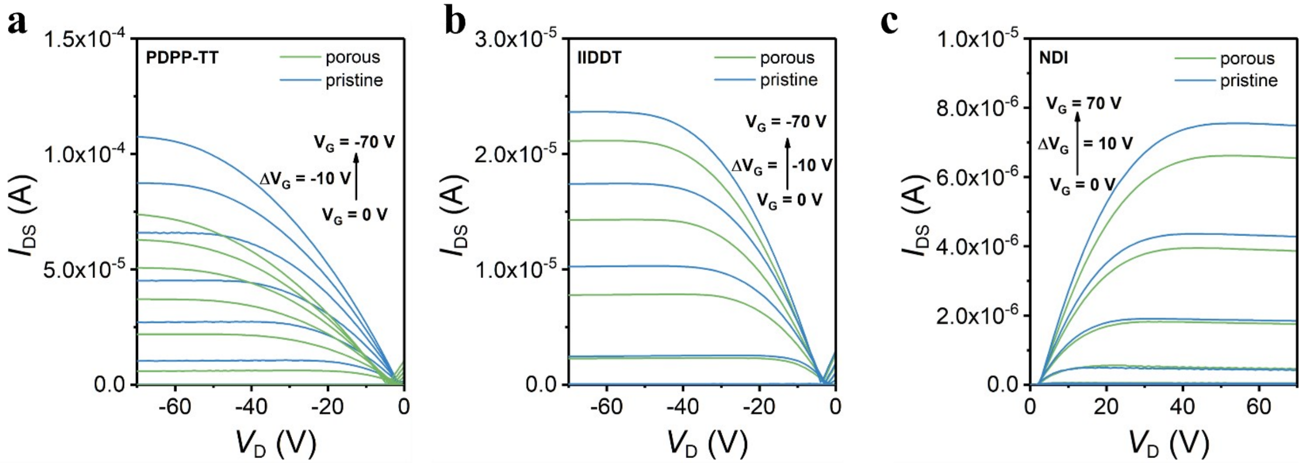

Fig. S8. Output characterization. OFET output curves for (a) PDPP-TT, (b) IIDDT and (c) NDI based devices.

Supplementary Note 1. The mobility calculation for OFET device with pristine and patterned OSC film.

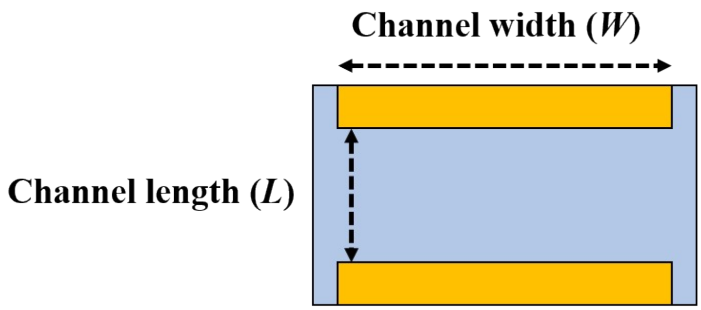

$$\mu = \frac{2L}{WC_i}\left(\frac{\partial\left(\sqrt{|I_D|}\right)}{\partial V_G}\right)^2$$

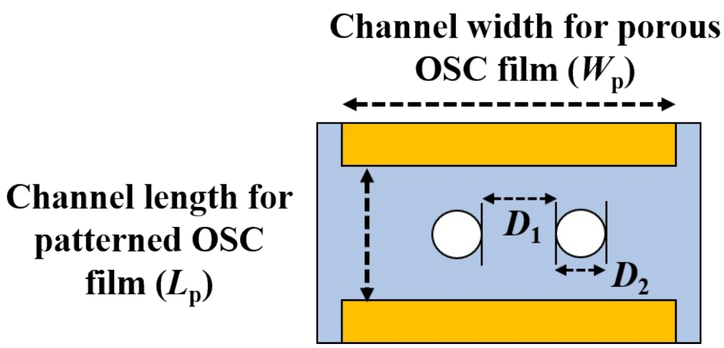

$$\mu_P = \frac{2L_P}{W_P C_i}\left(\frac{\partial\left(\sqrt{|I_D|}\right)}{\partial V_G}\right)^2$$

$$W_P = \frac{D_1}{D_2}W$$

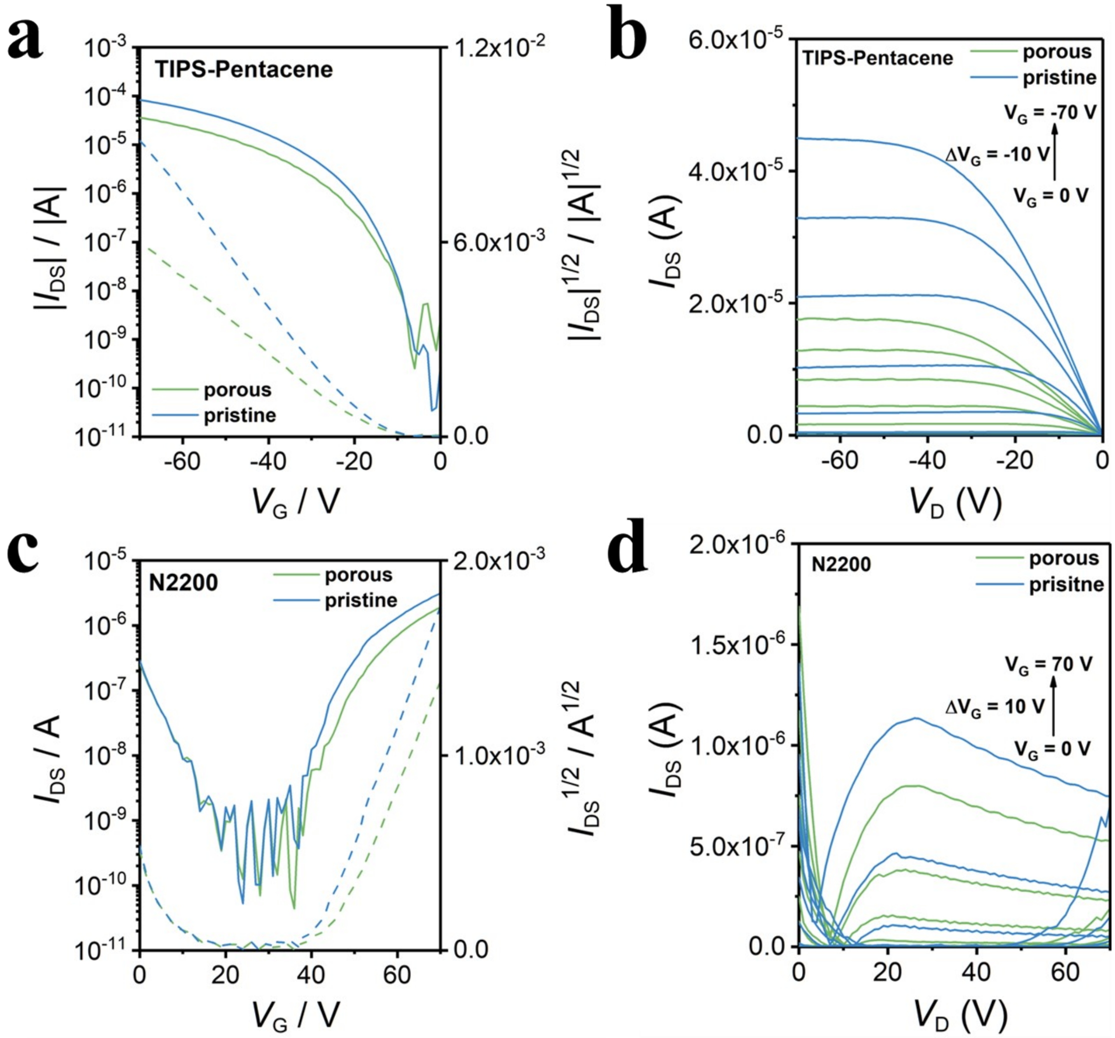

Fig. S9. Transfer and output curves of pristine and patterned films of (a,b) TIPS-Pentacene and (c,d) N2200.

Table S1. The estimated D_1, D_2, carrier mobility (μ), threshold voltage (V_{th}) and I_{on}/I_{off} values of the pristine and patterned TIPS-Pentacene and N2200 devices.

	Material	D_1 (μm)	D_2 (μm)	μ^a ($cm^2V^{-1}s^{-1}$)	V_{th} (V)	I_{on}/I_{off}
Pristine	TIPS-Pentacene	-	-	0.34 ± 0.010	-16.9	10^6
	N2200	-	-	0.085 ± 0.002	40.4	10^5
Porous	TIPS-Pentacene	1.149 ± 0.076	2.443 ± 0.113	0.32 ± 0.008	-17.5	10^5
	N2200	1.027 ± 0.060	2.637 ± 0.056	0.079 ± 0.002	45.1	10^5

[a]The effective mobilities were extracted from transfer curves measured from eight individual devices.

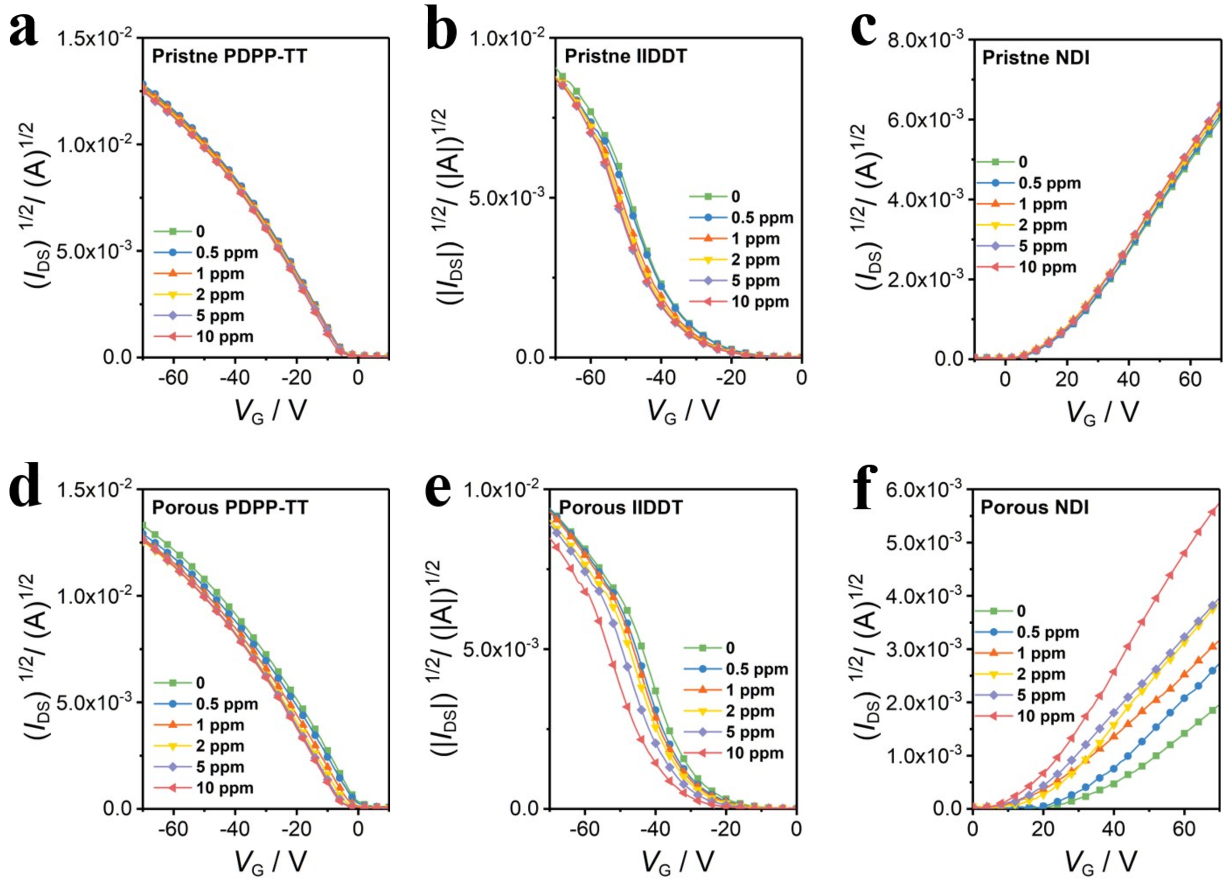

Fig. S10. Square root of drain current versus gate voltage plots at indicated NH_3 concentrations for (a,d) PDPP-TT, (b,e) IIDDT and (c,f) NDI based devices.

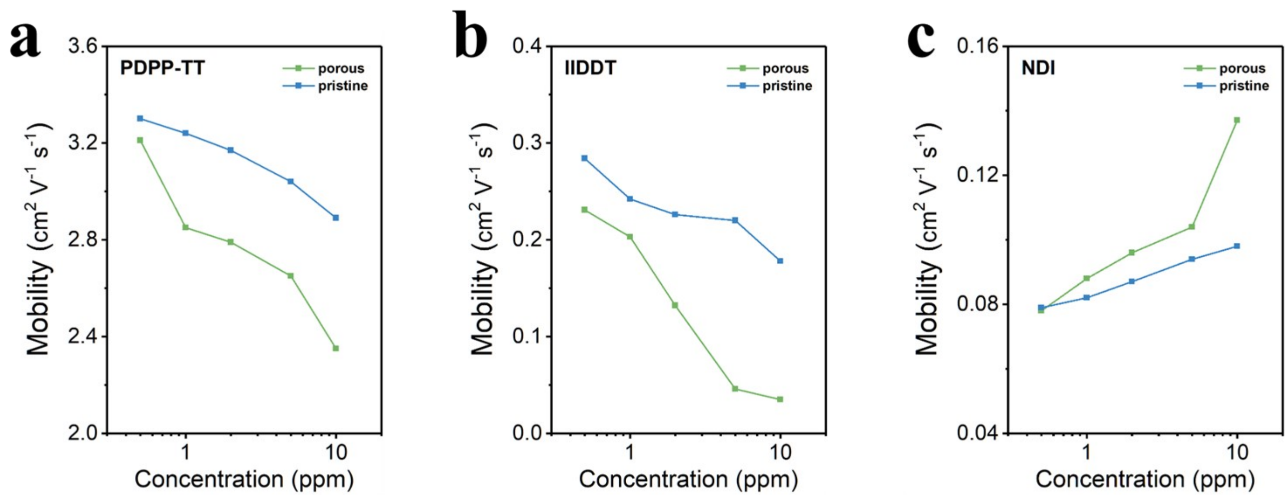

Fig. S11. Extracted mobility values of gas sensor devices as a function of NH_3 concentrations for (a) PDPP-TT, (b) IIDDT and (c) NDI materials.

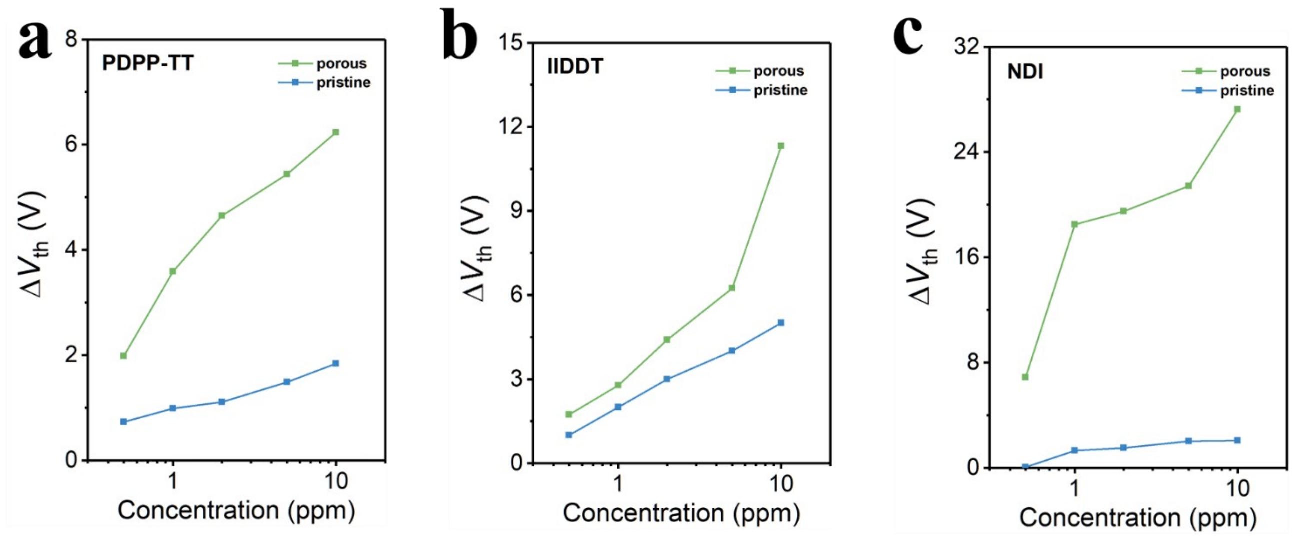

Fig. S12. Threshold voltage variations at indicated NH_3 concentrations for (a) PDPP-TT, (b) IIDDT and (c) NDI based devices.

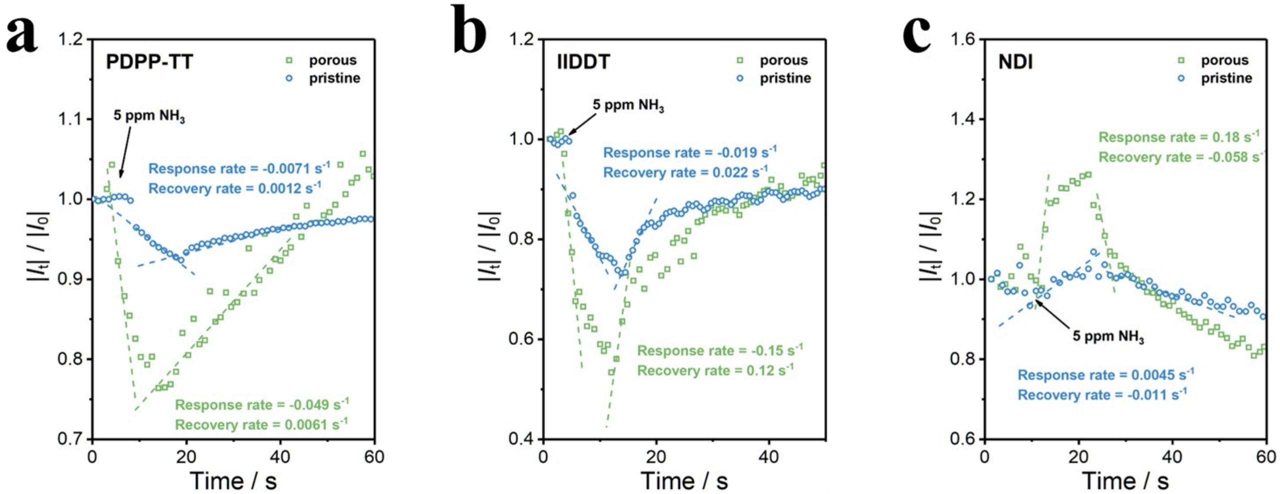

Fig. S13. Response and recovery rates for (a) PDPP-TT, (b) IIDDT, and (c) NDI based OFET gas sensors when exposed to 5 ppm NH_3.

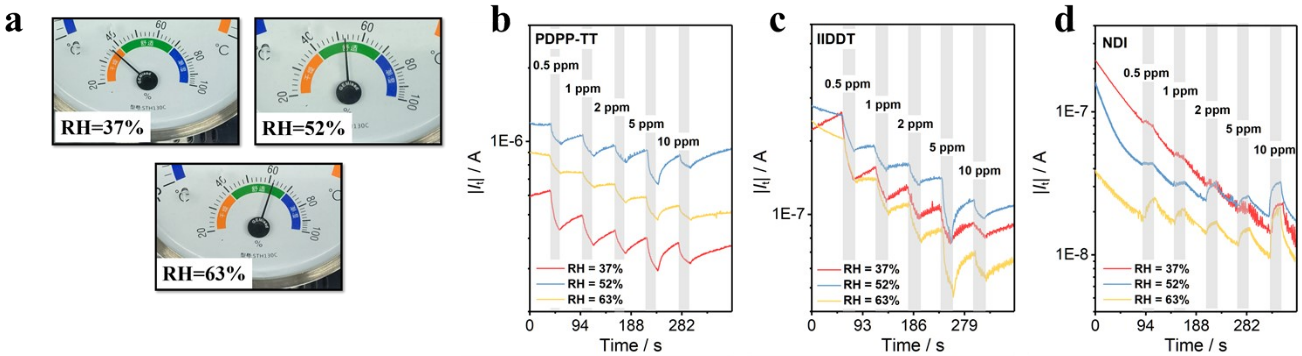

Fig. S14. (a) Photos of hygrometer with different relative humidity (RH) readings. The gas response of patterned OSC based OFET device was tested in different conditions with the RH of 37%, 52%, and 63%. (b-d) Drain current upon exposure to NH_3 of indicated concentration under various RH conditions for (b) PDPP-TT, (c) IIDDT and (d) NDI based devices.

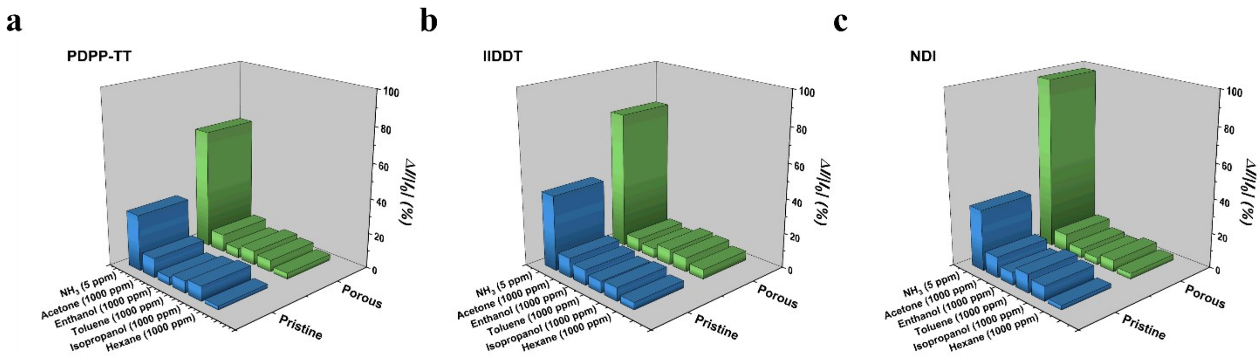

Fig. S15. Gas sensing sensitivities toward various gaseous analytes for (a) PDPP-TT, (b) IIDDT, and (c) NDI based devices. The concentration of gas analyte is 5 ppm, 1000 ppm, 1000 ppm, 1000 ppm, 1000 ppm, and 1000 ppm for NH_3, acetone, enthanol, toluene, isopropanol, and hexane, respectively.